Official journal of the American Society of Gene & Cell Therapy

MTOpen

AAV2/1 CD74 Gene Transfer Reduces β-amyloidosis and Improves Learning and Memory in a Mouse Model of Alzheimer's Disease

Tomomi Kiyota[1], Gang Zhang[1], Christine M Morrison[1], Megan E Bosch[1], Robert A Weir[1], Yaman Lu[1], Weiguo Dong[1] and Howard E Gendelman[1,2]

[1]Department of Pharmacology and Experimental Neuroscience, University of Nebraska Medical Center, Omaha, Nebraska, USA; [2]Department of Internal Medicine, University of Nebraska Medical Center, Omaha, Nebraska, USA

Modulation of the amyloid-β (Aβ) trafficking pathway heralds a new therapeutic frontier for Alzheimer's disease (AD). As CD74 binds to the amyloid-β precursor protein (APP) and can suppresses Aβ processing, we investigated whether recombinant adeno-associated virus (AAV) delivery of CD74 could reduce Aβ production and affect disease outcomes. This idea was tested in a mouse AD model. Cotransduction of AAV-tetracycline-controlled transactivator (tTA) and AAV-tet-response element (TRE)-CD74 resulted in CD74 expression, reduced Aβ production in mouse neurons containing the human APP with familial AD-linked mutations. Stereotaxic injection of AAV-TRE-GFP or CD74 into the hippocampi of an AD mouse, defined as a TgCRND8 × calmodulin-dependent protein kinase II derived promoter-tTA double-transgenic, reduced Aβ loads and pyramidal neuronal Aβ accumulation in the hippocampus. Immunofluorescent studies showed that APP colocalization with Lamp1 was increased in CD74-expressing neurons. Moreover, Morris water maze tasks demonstrated that mice treated with AAV-TRE-CD74 showed improved learning and memory compared to AAV-TRE-GFP control animals. These results support the idea that CD74-induced alteration of Aβ processing could improve AD-associated memory deficits as shown in mouse models of human disease.

Received 10 December 2014; accepted 23 July 2015; advance online publication 1 September 2015. doi:10.1038/mt.2015.142

INTRODUCTION

Alzheimer's disease (AD) is the most common form of cognitive impairment affecting the elderly. There is neither a cure nor an effective therapy for the progressive neurodegeneration that hallmarks AD. Neuropathologically, the disease is characterized by the presence of extracellular senile plaques and intraneuronal neurofibrillary tangles in affected brain tissue.[1] While neurofibrillary tangles consist of abnormally hyperphosphorylated microtubule associated protein tau, senile plaques are the aggregation of amyloid-β peptides (Aβ) in the extracellular space. Over the past decade, therapeutic efforts for AD were made through combating disease mechanisms including the clearance of Aβ. This was believed to be beneficial toward attenuating disease outcomes as Aβ induces neuroinflammation, consequent synaptic and neuritic injuries, tau hyperphosphorylation, and ultimately neuronal death.[2,3] In particular, immunotherapies that serve to clear Aβ deposits could improve AD-linked outcomes as were demonstrated in mouse models of human disease.[4,5] Nonetheless, both active and passive immunization showed disappointing results in clinical trials.[5,6] This suggested that removing Aβ, particularly extracellular deposits, may not directly lead to improved cognitive function. Thus, alternative strategies to treat the disease remain of critical importance to affect disease outcomes.

Aβ precursor protein (APP) is a type I membrane protein synthesized then modified posttranslationally in the endoplasmic reticulum and Golgi apparatus. APP is transported to cell surface by mechanisms analogous to other integral transmembrane proteins.[7] It's metabolism follows either a nonamyloidogenic or amyloidogenic pathway through α-secretase or by the β-site APP cleaving enzyme (BACE). Nonamyloidogenic processing predominantly occurs at the cell surface. α-secretase cleaves APP within the Aβ domain and produces a secreted (s)APPα large amino and small carboxyl (C)-terminal fragments (αCTF: C83). Amyloidogenic processing preferentially occurs in endosomes.[8] Recent studies demonstrate that APP is internalized through lipid rafts and clathrin-mediated endocytosis. BACE is internalized by ADP ribosylation factor 6 endosytosis then sorted to early endosomes (see review).[8] BACE processes APP to a soluble β-cleaved ectodomain (sAPPβ) and a C-terminal fragment (βCTF: C99).[9] The γ-secretase complex is responsible for the cleavage of βCTF generating Aβ, which is released to the extracellular space by fusion of multivesicular bodies with the plasma membrane or degraded during the endolysosomal pathway.[10,11] Importantly, endosomal alteration is an early event in AD progression, resulting in intraneuronal Aβ accumulation. In both animal models and human disease, intraneuronal accumulation of pathogenic Aβ42 correlates with synaptic dysfunction, cognitive impairment, and accelerated aging.[12,13] These suggest that Aβ trafficking pathways may be a therapeutic target to improve disease manifestations.

The chaperone CD74 (also known as invariant chain) is a nonpolymorphic glycoprotein. CD74 controls major

Correspondence: Tomomi Kiyota, Department of Pharmacology and Experimental Neuroscience, University of Nebraska Medical Center, 985930 Nebraska Medical Center, Omaha, Nebraska 68198-5930, USA. E-mail: tkiyota@unmc.edu

histocompatibility complex (MHC) class II protein trafficking and primes dendritic cells for antigen presentation.[14] CD74 also interacts with MHC class I (MHC I) in the endoplasmic reticulum of the dendritic cells, serving to mask MHC I and as a trafficking mediator towards endosome and endolysosomal compartments.[15] While CD74 is not principally expressed in neurons,[14] its expression is observed with neurofibrillary tangles in AD brain tissue.[16] Although CD74 binds to APP including APP FAD mutants and can suppress Aβ production shown in cell lines that overexpressed CD74 and APP, its role in disease pathogenesis is not yet defined.[17] Thus, the role CD74 plays in AD pathobiology and Aβ metabolism awaits further investigation.

To such ends, recombinant adeno-associated virus (AAV) serotype 2/1 containing CD74 or a green fluorescent protein (GFP) as a control regulated by the tetracycline transactivator (tTA) was employed to test how CD74 effects β-amyloidosis, Aβ neuronal trafficking and metabolism. APP Tg mice (TgCRND8 strain) mice were crossed with calcium-calmodulin-dependent kinase 2a (Camk2a) promoter derived tTA mice to generate the APP/tTA mice (defined as AD mice). These mice received intracranial AAV injections with subsequent neuropathological, biochemical, and behavioral analyses.

RESULTS

AAV-mediated CD74 expression

CD74 is expressed in antigen-presenting cells.[14] While AAV2/1 is tropic for neurons,[18,19] a physiological role for CD74 in neurons is unclear. Therefore, controlled CD74 expression and any resultant alteration in neuronal physiology were assessed. To achieve this, a Tet-Off system was employed where tetracycline-controlled transactivator (tTA) activated a tetracycline-response element (TRE)/minimal cytomegalovirus (CMV) promoter (**Figure 1a**). Neural progenitor cell (NPC)-derived neurons were cotransduced with AAV-TRE-GFP and AAV-tTA. GFP expression was subsequently increased in a dose-dependent manner. Such responses were suppressed by doxycycline (**Figure 1b**). At a dose of 1×10^9 of the AAV viral genome (vg), GFP was expressed 3 days after transduction and increased in a time-dependent manner (**Figure 1c,d**). CD74 expression was observed in NPC-derived neurons after cotransduction with AAV-TRE-CD74 and AAV-tTA. However, the level of CD74 expression was less than that observed with GFP (**Figure 1e**). To assess CD74 effects in neurons, we first measured cell viability using the 3-(4,5-dimethylthiazol-2-yl)-2,5-diphenyltetrazolium bromide (MTT) assay. AAV transduction of CD74 resulted in sustained cell viability when compared to control, tTA, or GFP cell groups

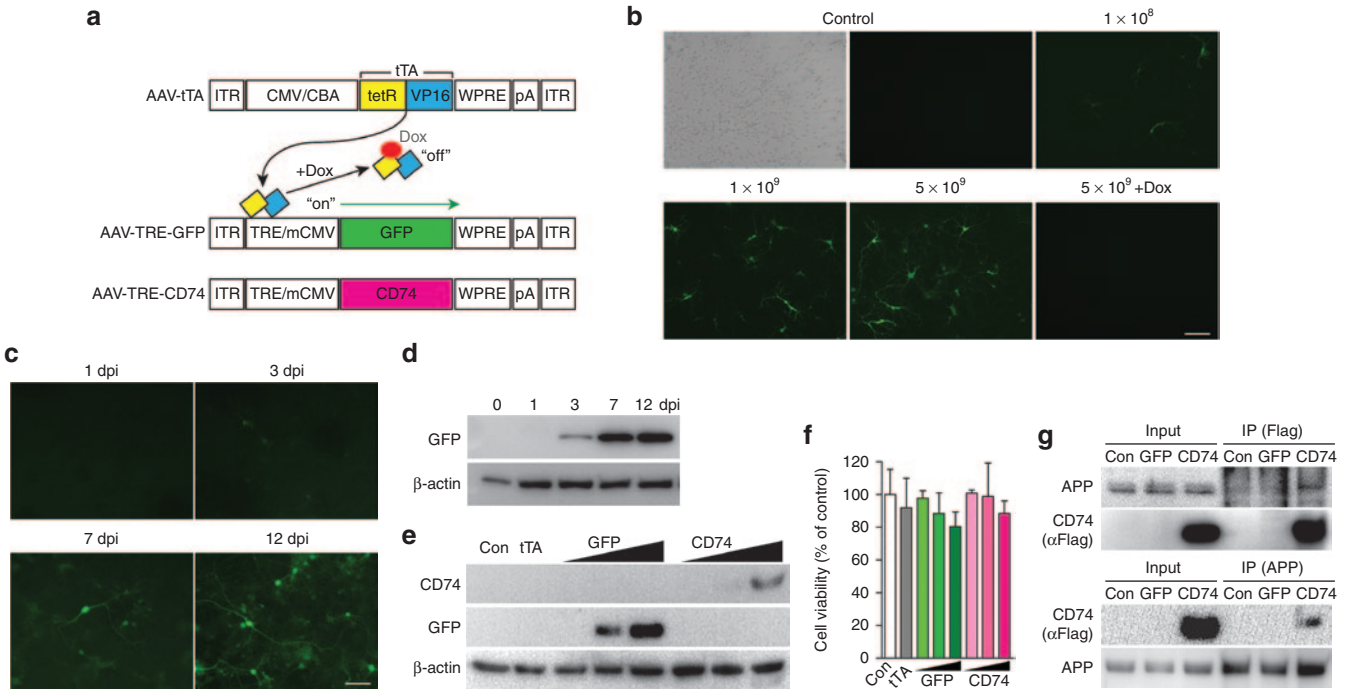

Figure 1 Optimization for AAV-TRE-GFP and CD74 *in vivo*. (**a**) Schematic for our tetracycline (tet)-controlled transactivator (tTA, composed of tet repressor (tetR)-VP16 fusion) regulatory system. tTA is expressed under the control of a cytomegalovirus/chicken β-actin hybrid promoter (CMV/CBA), and binds to tet-response element (TRE) to induce green fluorescent protein (GFP) or CD74 expression via the cytomegalovirus minimal promoter (mCMV). In presence of tet or its analogue doxycycline (Dox), tTA with Dox that binds to tetR is unable to bind to TRE, and GFP or CD74 transcription is inactive. ITR, inverted terminal repeats; WPRE, Woodchuck hepatitis post-transcriptional regulatory element; pA, bovine growth hormone polyadenylation site. (**b**) Titration of AAV-TRE-GFP (vg/2 × 10^5 cells/well in 24-well plates) in neural progenitor cell (NPC)-derived neurons (cotransduced with AAV-tTA at 1×10^9 vg for 7 days). Increasing infective dose shows increasing GFP expression. Dox treatment (1 μg/ml) completely inhibits GFP expression. (**c**) AAV-TRE-GFP transduced NPC-derived neurons (1×10^9 vg, cotransduced with AAV-tTA at 1×10^9 vg/2 × 10^5 cells/well in 24-well plates) show increased GFP expression over time course of 12 days. (**d**) In the same condition as in **c**, GFP expression is detectable at 3 days after transduction by immune blot. (**e**) Immune blots show expression of GFP and CD74 in NPC-derived neurons in a dose-dependent manner. (**f**) Overexpression of CD74 has no effect on cell viability as compared to GFP group. (**g**) Full-length APP is coimmunoprecipitated with CD74 and vice versa. Scale bar = 100 (**b**) or 50 μm (**c**). AAV, adeno-associated virus; APP, Aβ precursor protein; IP, immunoprecipitation; tTA, tetracycline transactivator.

(Figure 1f). We posited that this occurred despite CD74 binding to neuronal APP. In order to confirm that CD74 binding to APP occured, neurons were transduced with AAV2-flag-tagged-CD74. This was followed by infection with adenovirus expressing the human APP Swedish mutant (AdAPPsw), then cell lysates were subjected to immunoprecipitation (IP) (Figure 1g). CD74 interacted with mature APP. Further reciprocal IP confirmed that CD74 was coprecipitated with APP, indicating CD74 association with neuronal APP.

CD74 suppresses Aβ in neurons

CD74 overexpression decreases both Aβ40 and Aβ42 secretion from human embryonic kidney 293 APP cells.[17] To confirm a similar effect in NPC-derived neurons, we infected the neurons with AdAPPsw, followed by AAV transduction for 3 days (Figure 2a). AdAPPsw infection only, AdAPPsw and transduction of AAV-tTA, or AdAPPsw and transduction of both AAV-tTA and AAV-TRE-GFP showed significant production of Aβ40 and Aβ42 compared to adenovirus expressing GFP alone. Transduction of AAV-tTA and AAV-TRE-CD74 reduced both Aβ40 and Aβ42 production (48 and 54% reductions for Aβ40 and Aβ42, respectively, Figure 2b,c). These data demonstrate that CD74 inhibits neuronal Aβ secretion.

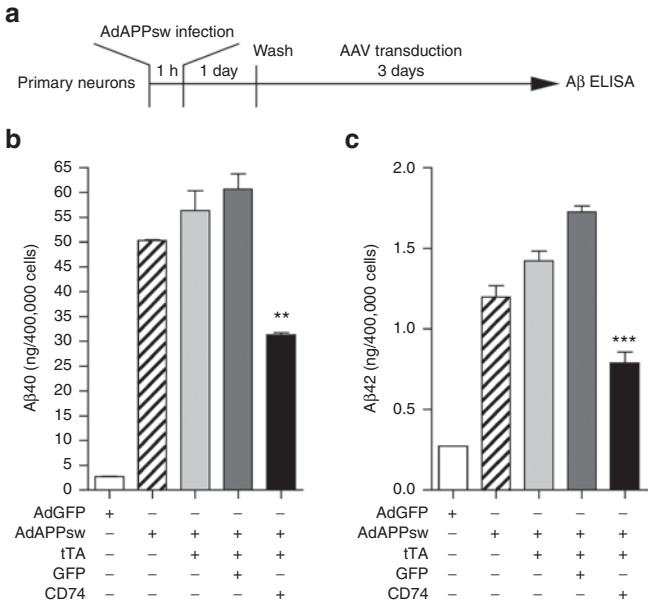

Figure 2 CD74 suppresses Aβ production from neural progenitor cell (NPC)-derived cultured neurons. (**a**) Experimental designs for *in vitro* Aβ production assay. NPC-derived neurons (4×10^5 cells/well in 24-well plates) were infected with adenovirus expressing APPsw (AdAPPsw) or green fluorescent protein (GFP) (AdGFP), followed by transduction of AAV-TRE-GFP or CD74 (2×10^9 vg, cotransduced with AAV-tTA at 2×10^9 vg) for 3 days. Neuron culture media were subjected to Aβ40 or Aβ42 ELISA. (**b**,**c**) NPC-derived neurons were infected with adenovirus expressing GFP or APPsw (AdGFP or AdAPPsw), followed by transduction of AAV-tTA only or plus AAV-TRE-GFP or CD74. Aβ40 (**b**) or Aβ42 (**c**) production was quantified. Bars represent mean ± standard error of the mean. ** or *** denotes $P < 0.01$ or 0.001 versus AdAPPsw only, plus AAV-tTA or plus AAV-TRE-GFP as determined by one-way analysis of variance, Newman-Keuls *post hoc* test. AAV, adeno-associated virus; ELISA, enzyme-linked immunosorbent assay; TRE, tet-response element; tTA, tetracycline (tet)-controlled transactivator.

CD74 attenuates hippocampal Aβ in AD mice

To further elucidate the effect of CD74 on β-amyloidosis, we injected AAV-TRE-GFP or -CD74 (1×10^9 vg/2 µl per shot) bilaterally into the hippocampi of the AD mice at 2 months of age. Following the sacrifice of the AD and control animals at 6 months of age, the brains were secured and neuropathological analyses performed (Figure 3a). At the terminal time point, GFP and CD74 expression in the hippocampus were confirmed (Figure 3b–d). Efficient GFP expression was observed in AAV-TRE-GFP-injected mice. CD74 was expressed at a slightly higher level in AAV-TRE-CD74-injected mice than what was observed in the other groups (Figure 3b,c). Fluorescent analyses showed that robust GFP expression was retained in the hippocampus injected with AAV-TRE-GFP, notably in pyramidal neurons and neuropils in Cornet d'Ammon (CA) 1, CA2, and CA3. AAV-TRE-CD74 injection resulted in limited but pyramidal neuron-specific expression of CD74 in CA1-3 of the hippocampus. No neuronal expression of CD74 was observed in uninjected Tg and non-Tg controls (Figure 3d).

Since CD74 expression significantly reduces Aβ secretion in cell-based assays, we tested whether the observed results translate to the mouse brain (Figure 4a). The AAV-TRE-CD74-injected group showed significant reductions in hippocampal Aβ loads and number of Aβ plaques (38 and 17% reductions when compared to AAV-TRE-GFP group, Figure 4b,c), demonstrating the anti-β-amyloidosis effect of CD74 *in vivo*. Confocal microscopy analyses demonstrated that intraneuronal accumulation of Aβ was spread through cell bodies of pyramidal neurons in AAV-TRE-GFP-injected group, but Aβ immunoreactivity was limited, reduced and effectively colocalized with CD74 expression in AAV-TRE-CD74–injected group (82% reduction when compared to AAV-TRE-GFP group, Figure 4d,e). To quantify the levels of Aβ40 and Aβ42, hippocampal homogenates were separated as extracellular (extracellular Aβ plaques), intracellular (intracellular Aβ), and membrane-enriched fractions.[20] Aβ enzyme-linked immunosorbent assay (ELISA) showed decreased Aβ40 and Aβ42 levels in both fractions (extracellular Aβ—13 and 14% reduction for Aβ40 and Aβ42, intracellular levels—42 and 37% reduction for Aβ40 and Aβ42, respectively when compared to AAV-TRE-GFP group, Figure 4f–i). The data shows correlations between pathological and biochemical evaluations.

CD74 overexpression changes APP metabolism in the mouse AD hippocampus

To determine how CD74 affects Aβ production, membrane-enriched fractions of hippocampal proteins were subjected to immunoblot tests using APP C-terminal antibodies to assess APP processing (Figure 5a). Surprisingly, full-length APP was reduced by 19% by CD74 overexpression when compared to the AAV-TRE-GFP-injected group (Figure 5b). βCTF and αCTF were also reduced by 47 and 33% (Figure 5c,d). These data suggest that CD74 reduces Aβ production by modification of APP metabolism. To further explore the mechanism underlying the APP metabolism in neurons, we investigated endosomal and lysosomal trafficking. NPC-derived neurons were transduced with AAV-tTA, AAV-TRE-APPsw, and AAV-TRE-GFP or CD74, and immunofluorescence was performed

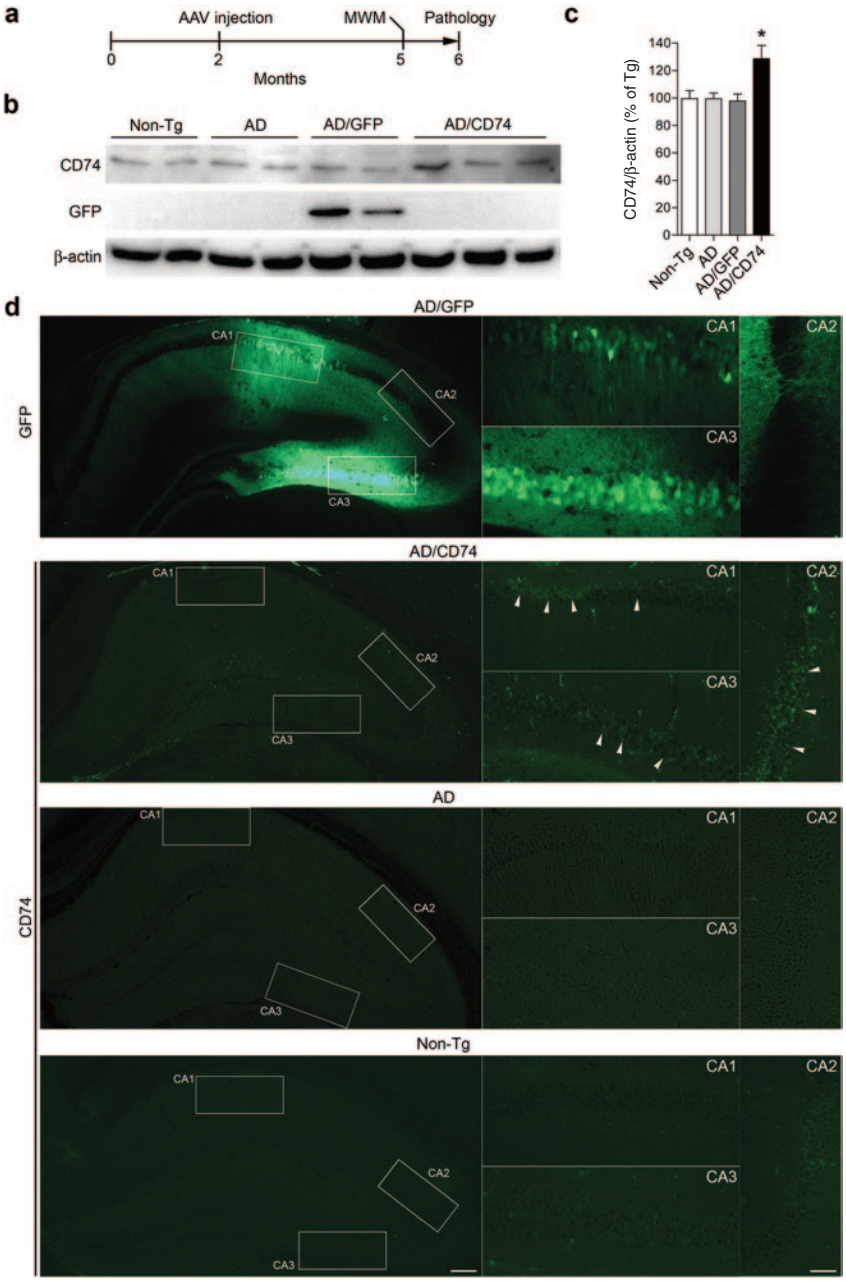

Figure 3 CD74 expression in the mouse hippocampus. (**a**) Experimental design. Alzheimer's disease (AD) mice received bilateral hippocampal injection of AAV-TRE-GFP or AAV-TRE-CD74 at 2 months of age, and were tested by Morris water maze task at 5–6 months of age. Non-tg mice served as positive control for spatial learning memory. Mice were sacrificed at 6 months of age for neuropathological analyses. (**b**) Immune blots of green fluorescent protein (GFP) and CD74 in membrane-enriched fraction of the mouse hippocampus after injection of AAV-TRE-GFP or CD74. (**c**) Quantification of CD74 expression ($n = 6$). Bars represent mean ± standard error of the mean. * denotes $P < 0.05$ as determined by one-way analysis of variance, Newman-Keuls *post hoc* test. (**d**) Fluorescent images of GFP in the AAV-TRE-GFP or CD74-injected hippocampus. AD (uninjected) and non-Tg serve as a negative control. Scale bar = 300 (low) or 100 μm (high magnification). AAV, adeno-associated virus; MWM, Morris water maze; TRE, tet-response element.

with antibodies to Rab5 (for early endosomes), Rab7 (for late endosomes), and Lamp1 (for lysosomes). Confocal microscopy demonstrated that CD74 overexpression resulted in no significant changes in APP expression and Rab colocalization (**Supplementary Figure S1a,b**). However, colocalization of Lamp1 with APP was increased in CD74-overexpressed neurons over control and GFP groups (**Figure 6**), suggesting that CD74 promotes lysosome-mediated APP degradation in neurons.

CD74 restores spatial memory

Next, we tested the role for CD74 in memory function. AAV-injected AD mice were subjected to the Morris water maze task (**Figure 7a**). This test was used to assess memory acquisition. Following the acquisition phase, a 1-day probe test was used to determine memory retention of the mice at 5 to 6 months of age (**Figure 7b**). Uninjected and AAV-TRE-GFP-injected AD groups showed impaired learning and memory acquisition as compared to non-Tg control and AAV-TRE-CD74-injected AD groups

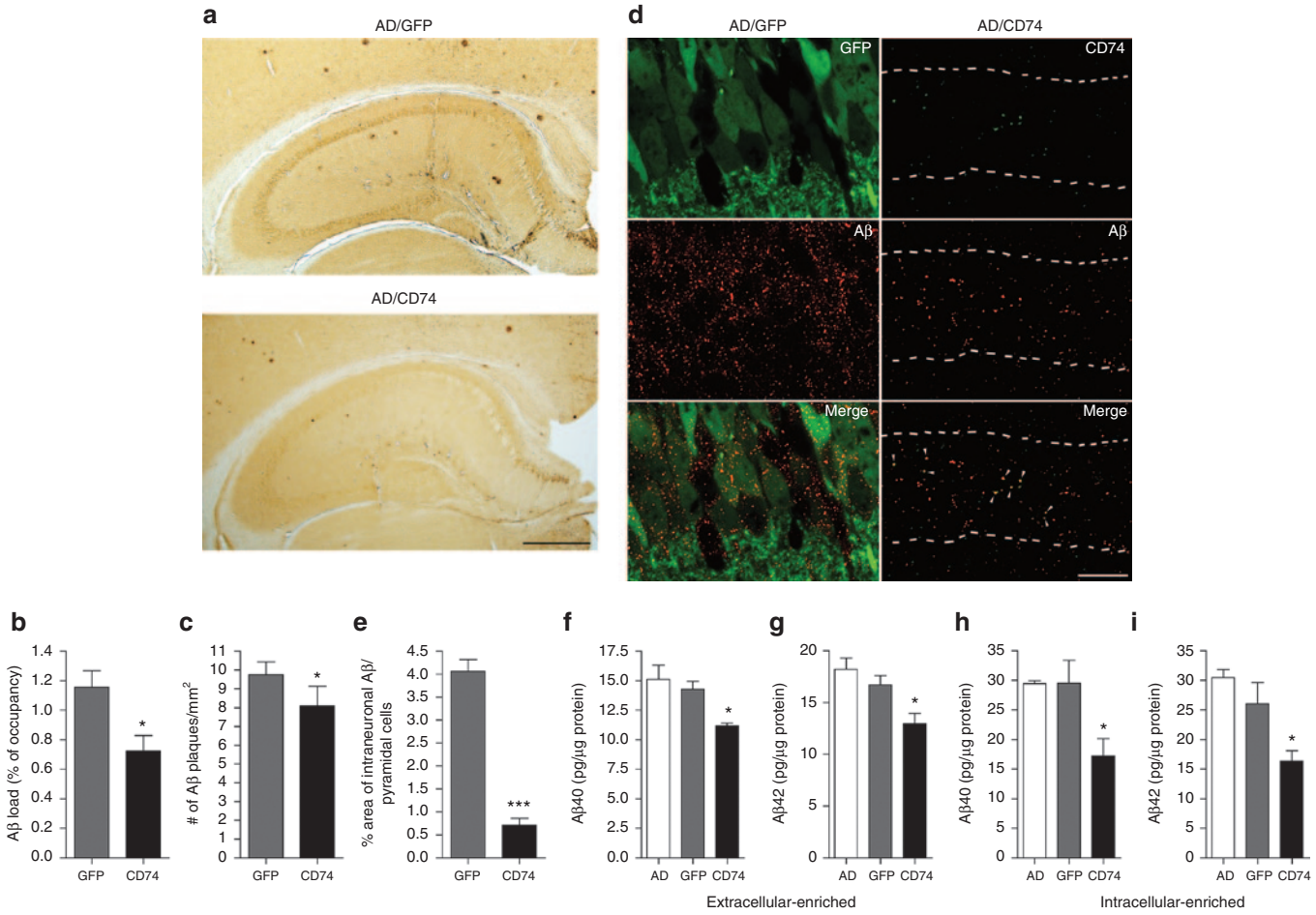

Figure 4 CD74 attenuates Aβ loads in the hippocampus of Alzheimer's disease (AD) mice. (**a**) Representative images of Aβ staining in the hippocampus of AAV-TRE-GFP or AAV-TRE-CD74-injected AD mice. Scale bar = 500 μm. (**b,c**) Quantification of total Aβ loads (**b**) and number of Aβ plaques (**c**) in the hippocampal region ($n = 6$ per group, 10 sections per brain). (**d**) Confocal microscopy shows intraneuronal accumulation of Aβ (red) in GFP or CD74-positive neurons (green). Numbers of Aβ are observed in GFP-positive neurons but not in CD74-positive neurons. CD74 expression is colocalized with Aβ (arrowheads). Pyramidal cell layer is indicated with broken lines. 630× magnification. Scale bar = 10 μm. (**e**) Quantification of intraneuronal Aβ in pyramidal neurons ($n = 10$). (**f–i**) The levels of Aβ40 (**f,h**) and Aβ42 (**g,i**) in extracellular (**f,g**) and intracellular (**h,i**)-enriched fractions were measured by human Aβ40- and Aβ42-specific enzyme-linked immunosorbent assays ($n = 8$). Bars represent mean ± standard error of the mean. * denotes $P < 0.05$ as determined by Student's *t*-test. AAV, adeno-associated virus; GFP, green fluorescent protein; TRE, tet-response element.

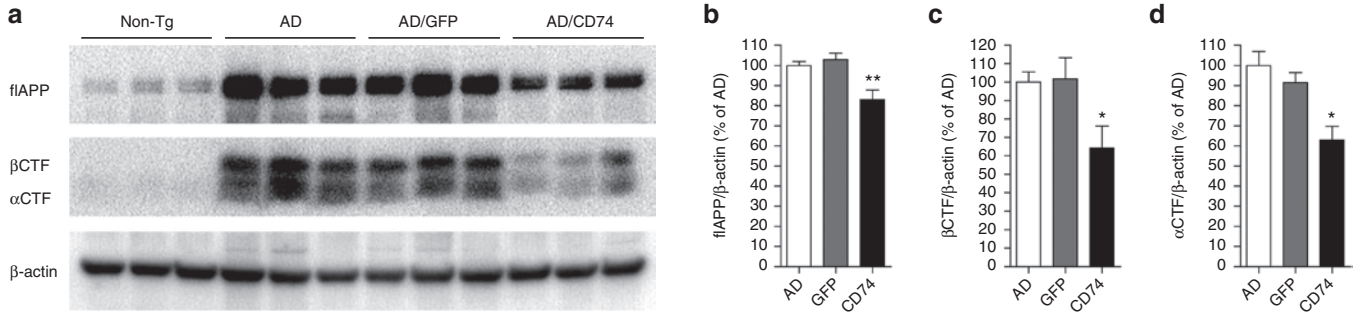

Figure 5 CD74 decreases full-length, C99 and C83 CTF human amyloid-β precursor protein (APP) in the hippocampus of Alzheimer's disease (AD) mice. (**a**) Immune blots of full-length (flAPP), C99 βCTF and C83 αCTF human APP in membrane-enriched fraction of the mouse hippocampus after injection of AAV-TRE-GFP or CD74. (**b–d**) Quantification of flAPP (**b**), C99 βCTF (**c**), and C83 αCTF (**d**) in the hippocampus ($n = 8$). Bars represent mean ± standard error of the mean. * or ** denotes $P < 0.05$ or 0.01 versus AD mice or AAV-TRE-GFP-injected group as determined by one-way analysis of variance, Newman-Keuls *post hoc* test. AAV, adeno-associated virus; CTF, carboxyl-terminal fragment; GFP, green fluorescent protein; TRE, tet-response element.

(Figure 7a). This included trends of few annulus crossings in the target quadrant, which contained a submerged platform observed during the memory acquisition phase (Figure 7c), and no quadrant preference (Figure 7d). However, AAV-TRE-CD74-injected AD groups showed better memory acquisition including an increased number of annulus crossings and quadrant preference

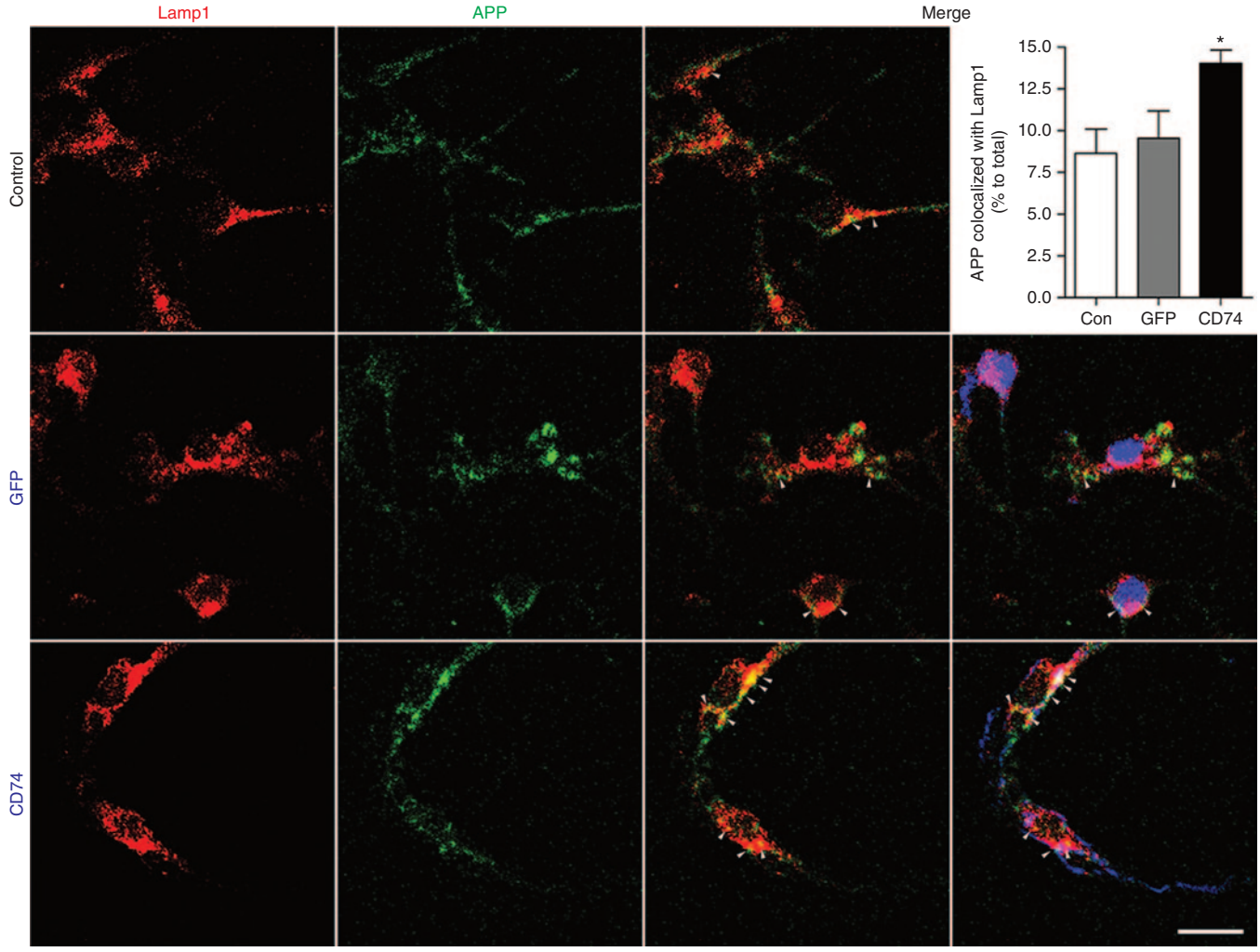

Figure 6 Subcellular localization of amyloid-β precursor protein (APP) and Lamp1 in CD74-overexpressing neurons. Confocal microscopy shows cellular localization of Lamp1 lysosomal compartment (red), APP (green) and GFP or CD74 (pseudo-colored blue). Merged images of Lamp1 and APP with or without GFP/CD74 are shown. APP co-localization with Lamp1 (arrowheads) was quantified by ImageJ with a colocalization plugin (n = 10). Scale bar = 10 µm. GFP, green fluorescent protein.

(**Figure 7c**,**d**). Average swim speeds were unchanged between groups, ruling out the possibility of difference in motor function (**Figure 7d**). This data further supports a role for CD74 in learning and memory.

CD74 suppresses Aβ production in human neurons

Finally, we tested if CD74 could advantageously reduce Aβ production in primary human neurons. The neurons were transduced with AAV-tTA combined with AAV-TRE-GFP or AAV-TRE-CD74 for 3 days. Cultured media were tested with Aβ40 and Aβ42 ELISA to quantify endogenous human Aβ levels. Cotransduction of AAV-tTA and AAV-TRE-CD74 reduced both Aβ40 and Aβ42 production (by 23 and 35% reductions, respectively) when compared to AAV-tTA and AAV-TRE-GFP groups (**Figure 8a**,**b**).

DISCUSSION

It is widely accepted that Aβ can induce neuroinflammation, synaptic and neuritic injuries, hyperphosphorylation of tau, and subsequent neuronal cell death.[2,3] Thus, the notion that Aβ removal can improve disease manifestations is plausible for further study and the need for the development of therapeutics is both timely and important. Indeed, anti-inflammatory drugs, amyloid degradation enzymes, and active/passive immunizations are all receiving a great deal of attention.[21–24] Limitations with such treatment strategies are notable as extracellular senile plaques once considered hallmarks of AD are not specific as cognitively normal individuals possess amyloid brain deposits at necropsy.[25,26] One may expect that intraneuronal accumulation of Aβ, rather than extracellular deposits, is critical for disease progression.[27,28] These findings led our laboratories to pursue targets shifted to intracellular pathways. We now posit that Aβ trafficking pathway may be one of several new therapeutic frontiers to combat β-amyloidosis.

CD74 is expressed principally in antigen-presenting cells such as B cells, monocytes, macrophages and dendritic cells.[14] CD74 controls the trafficking of MHC II for antigen presentation, and it serves as a mask and a trafficking mediator for MHC I to endosome and endolysosomal compartments.[15] It also influences macrophage migration inhibitory factor that is involved in cell proliferation and

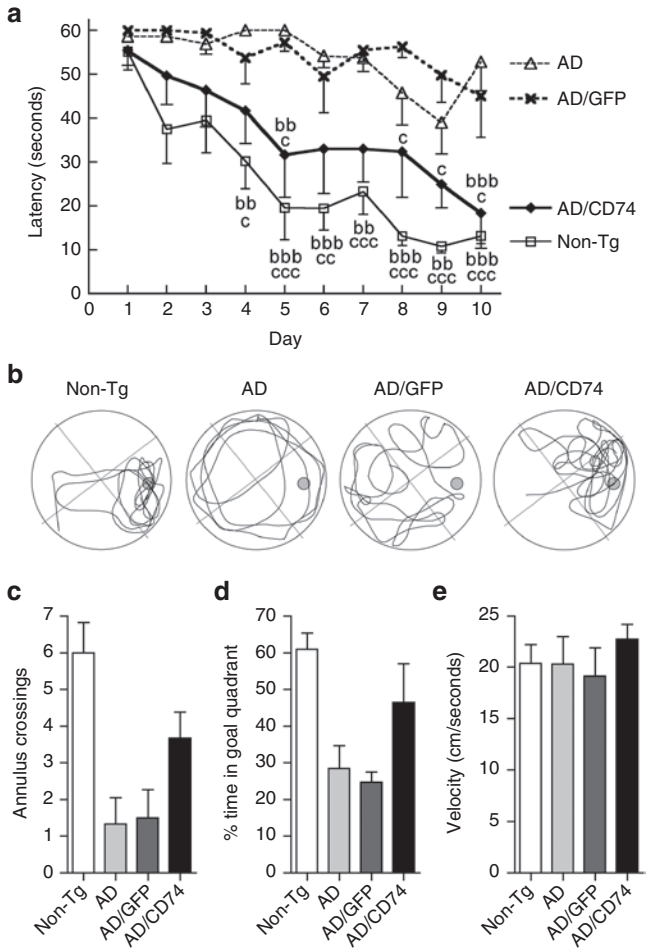

Figure 7 Morris water maze (MWM) task reveals improved memory acquisition and retention in AAV-TRE-CD74-injected Alzheimer's disease (AD) mice. (**a**) While Alzheimer's disease (AD) and AAV-TRE-GFP-injected AD mice show statistically higher escape latencies as compared to non-Tg group, AAV-TRE-CD74-injected AD mice show fewer escape latencies at 5–6 months of age in MWM acquisition phase where escape latency during a 1-minute trial was measured. (**b**) Representative swim paths of non-Tg, uninjected AD, AD/GFP, and AD/CD74 mice during a one-time probe trial after memory acquisition. (**c**,**d**) Number of annulus crossings (**c**) and duration spent in the goal quadrant between groups (**d**) were analyzed as a MWM retention phase. While uninjected and AAV-TRE-GFP-injected AD mice show a trend to decrease both number of annulus crossings (**c**) and percent search time (**d**), CD74-injected AD mice show improved memory retention. (**e**) Measurement of average swimming speed of animals. Average swimming speeds are unchanged between groups. Data are presented as mean ± standard error of the mean. $^{c}P < 0.05$, $^{bb,\ cc}P < 0.01$, $^{bbb,\ ccc}P < 0.001$, $^{bb,\ bbb}$ vs AD mice, $^{c,\ cc,\ ccc}$ versus AAV-TRE-GFP-injected AD mice, two-way analysis of variance, Bonferroni *post hoc* test. AAV, adeno-associated virus; GFP, green fluorescent protein; TRE, tet-response element.

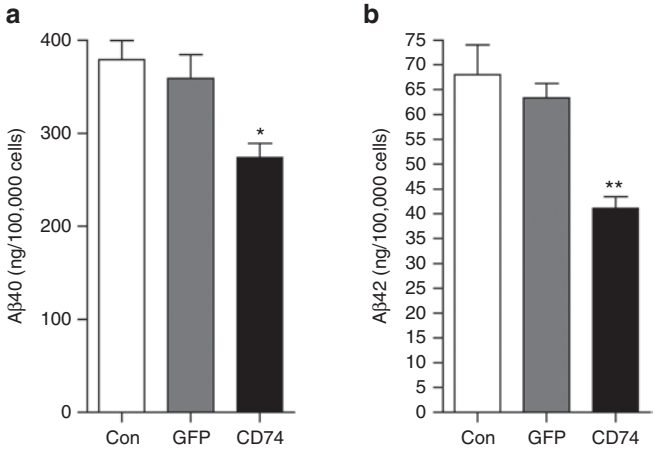

Figure 8 CD74 suppresses Aβ production from cultivated human neurons. (**a**,**b**) Human neurons (1×10^5 cells/well in 48-well plates) were transduced with AAV-tTA at 0.5×10^9 vg combined with AAV-TRE-GFP or CD74 (0.5×10^9 vg) for 3 days. Neuron culture media were subjected to Aβ40 (**a**) or Aβ42 (**b**) enzyme-linked immunosorbent assay tests. Bars represent mean ± standard error of the mean. * or ** denotes $P < 0.05$ or 0.01 versus control or plus AAV-TRE-GFP as determined by one-way analysis of variance, Newman-Keuls *post hoc* test. AAV, adeno-associated virus; GFP, green fluorescent protein; TRE, tet-response element; tTA, tetracycline transactivator.

survival.[29,30] The role of CD74 in neurons was previously unknown. We now show that CD74 is expressed in NPC-derived neurons transduced with both AAV-tTA and AAV-TRE-CD74. Overexpression of CD74 in neurons did not affect cell viability nor expression of endolysosomal components when compared to control and GFP groups. In addition, expression level of CD74 was low as compared to that of GFP, even if the similar amounts of AAVs were employed *in vitro* transduction. Hippocampal AAV-TRE-CD74 injection did not show robust expression of CD74. Instead limited and appropriately regulated expression in pyramidal neurons was observed as targeted. These results suggest that "artificially" expressed CD74 is quickly turned over and not toxic during CD74 metabolism.

In human AD brains, CD74 is observed in pyramidal neurons colabeled with neurofibrillary tangles.[16] This may seem an apparent paradox based on our current observations. Indeed, CD74 could inhibit Aβ production and circumvent β-amyloidosis, if neuronal CD74 in AD brains acts as the overexpressed CD74 in their mouse counterparts in this study. Significant increases in CD74 is present based on AD severity.[16] Therefore, levels of CD74 in AD brains might be a compensatory response to disease progression. If this is correct, CD74 would not be effective to treat later AD stages.

Interestingly, chronic overexpression of CD74 reduced full-length APP level in the mouse brain. This was not observed in *in vitro* cell transfection system.[17] In this study, CD74 reduced Aβ, αCTF, and βCTF in the hippocampus. APP takes either α-secretase or BACE-mediated processing for its metabolism where the former occurs at the cell surface but the latter occurs in endosomes.[8] Thus, CD74 overexpression may affect both APP trafficking including posttranslational modification and endosomal pathway of βCTF. Our *in vitro* study showed that CD74 associates with APP and vice versa. Overexpression of CD74 did not affect expression of endolysosomal components, but increased colocalization of APP with Lamp1, suggesting promotion of lysosomal-mediated APP degradation and metabolism by CD74, and potential mechanism of reduced Aβ production as observed in pyramidal neurons injected with AAV-TRE-CD74.

Overall, we now demonstrate that recombinant CD74 overexpression results in reduced Aβ production in both mouse and human cultured neurons. AAV-TRE-CD74 injection ameliorates AD pathobiology including β-amyloidosis and impairments in learning and memory in the mouse brain. These effects are caused by reduction of both APP and Aβ, potentially through lysosomal

degradation pathways where APP is directed as a consequence of CD74 overexpression. Taken together, these findings support the idea that CD74 has new therapeutic potential to treat AD.

MATERIALS AND METHODS

Plasmid construction and AAV2/1 generation. pAAV2-TRE-MCS-WPRE (AAV2 inverted terminal repeats flanking TRE/minimal CMV promoter, multiple cloning site (MCS), and Woodchuck hepatitis post-transcriptional regulatory element, and the bovine growth hormone polyadenylation site), and pAAV2-TRE-GFP were constructed as previously described.[28] To construct pAAV2-CMV/CBA-tTA, a polymerase chain reaction (PCR) fragment containing tTA was amplified using the primers: Fw: 5′-GGCGGATCCGCCACCATGTCTAGATTAGATAAAAG-3′, Rev: 5′-TAGCTCGAGCT-ACCCACCGTACTCGTCAATTC-3′ and pUHD15-1 (a kind gift from Dr. Kay-Uwe Wagner at the University of Nebraska Medical Center) as a template DNA, digested with *Bam* HI and *Xho* I and inserted into the MCS of pAAV2-CBA-MCS-WPRE. For pAAV2-TRE-CD74 construction, pCMV-SPORT6 containing murine CD74 coding sequence (Open Biosystems clone 6530802) was digested with *Eco* RI and *Not* I and inserted into the MCS of pAAV2-TRE-MCS-WPRE. For pAAV2-CBA-MCS-Flag-WPRE construction, a PCR fragment containing 3× flag was amplified using the primers: Fw: 5′-GCAACGTGCTGGTTATTGTG-3′, Rev: 5′-AAATAAGCTTATTTGTCGTCATCATCCTTATAG-3′ and pShuttle-IRES-hrGFP-1 (Agilent Technologies, Santa Clara, CA) as a template DNA, digested with *Nhe* I and *Hind* III and inserted into the MCS of pAAV2-CBA-MCS-WPRE. For pAAV2-Flag-tagged-CD74 construction, a PCR fragment containing CD74 was amplified using the primers: Fw: 5′-GGCGGATCCGCCACCATGGATGACCAACGCGACCT-3′, Rev: 5′-CTGCTCGAGGGTGACTTGACCCAGTT-3′ and clone 6530802 as a template DNA, digested with *Bam* HI and *Xho* I and inserted into the MCS of pAAV2-CBA-MCS-Flag-WPRE. To construct pAAV2-TRE-APPsw, a PCR fragment containing APPsw was amplified using the primers: Fw: 5′-ATTTGCTAGCCACCATGCTGCCCGGTTT-3′, Rev: 5′-CTAGAAGCTTCTAGTTCTGCATCTGCTCAAAGAAC-3′ and adenoviral DNA extracted from AdAPPsw as a template DNA, digested with *Bam* HI and *Hind* III and inserted into the MCS of pAAV2-TRE-MCS-WPRE. AAV-293 cells (#240073, Agilent Technologies) were cotransfected with *cis* plasmid pAAV2-CMV/CBA-tTA, pAAV2-TRE-GFP, or pAAV2-TRE-CD74 with an AAV1 *trans* plasmid p5E18RXC1 and a helper plasmid pAdΔF6 (obtained from University of Pennsylvania Gene Therapy Program) to produce AAV-tTA, AAV-TRE-GFP and AAV-TRE-CD74. Cells were harvested, AAVs were purified and titration were performed as described previously.[31,32]

NPC cultivation. NPCs were prepared using NeuroCult Proliferation Kit (StemCell Technologies, Vancouver, BC, Canada) according to manufacturer's instruction. In brief, mouse cortices were dissected at embryonic day 14 and meninges were removed in ice-cold phosphate buffered saline (PBS) with 2% glucose. The cortices were mechanically dissociated, filtered with a 40 μm-cell strainer and cultured as neurospheres for 3–5 days in NeuroCult Proliferation media with epidermal growth factor (20 ng/ml). The neurospheres were collected and dissociated to single cells using a NeuroCult Chemical Dissociation Kit (StemCell Technologies, Vancouver, BC, Canada). The cells were seeded into poly-D-lysine (100 μg/ml) and laminin (15 μg/ml; Sigma-Aldrich, St. Louis, MO)-coated tissue culture plates. The proliferation media were exchanged with Neurobasal media containing B-27 supplement and 1× penicillin/streptomycin for differentiation.

Human neuron cultivation. Human neurons were isolated from fetal brain tissue cortices as previously described.[33] Cells were plated onto poly-D-lysine-coated 48-well plates at a density of 1×10^5 cells/well in Neurobasal media. A half volume of media was exchanged with fresh media every 3–5 days for 2 weeks. AAV transduction was performed as described above.

AAV transduction. Differentiated NPC (24-well) seeded at a density of 200,000 or 400,000 cells were transduced with AAVs in 200 μl Neurobasal media, then 300 μl fresh media were added 24 hours after transduction. A half volume of media was exchanged with fresh media on the following day and every 2–3 days. Brightfield and fluorescence images were captured using DP Controller and DP Manager with a digital camera DP71 (Olympus, Orangeburg, NY) attached to a Nikon Eclipse TE300 inverted microscope (Nikon, Melville, NY). Cells were harvested using ice-cold radioimmunoprecipitation assay buffer (Thermo Fisher Scientific, Waltham, MA) with protease inhibitor cocktail (Sigma, St Louis, MO) at end points. Protein concentrations were determined using a Micro BCA Protein Assay (Thermo Fisher Scientific).

MTT assay. Differentiated NPCs (96-well) were seeded at a density of 50,000 cells were transduced with indicated amounts of AAVs in 100 μl Neurobasal media for 24 hours, then 100 μl fresh media were added. A half volume of media was exchanged with fresh media on the following day after transduction. Cells were incubated with 10 μl of MTT (ATCC 30-1010K) for 4 hours at 37 °C. Media were aspirated from each well and 50 μl of dimethyl sulfoxide was added to dissolve the formazan crystals, and absorbance was measured using a plate reader at 570 nm.

Recombinant adenovirus generation and infection. Recombinant adenoviruses expressing GFP and APPsw (coexpressing GFP) were generated using AdEasy XL Adenoviral Vector System (#240010, Agilent Technologies), pShuttle-IRES-hrGFP-1 vector (#240081, Agilent Technologies) and pAdTrack-APPsw (a kind gift from Dr. Tsuneya Ikezu at Boston University).[34] Viral titer was measured using AdEasy Viral Titer Kit (#972500, Agilent Technologies). Differentiated NPCs or human neurons were infected with recombinant adenovirus expressing GFP or APPsw (MOI = 10) in 100 μl fresh Opti-MEM (Life Technologies, Carlsbad, CA) for 1 hour, followed by washing with PBS, 1-day incubation in Neurobasal media and AAV transduction for 3 days. The media were subjected to Aβ40 and 42 ELISA (Life Technologies).

Transgenic mice. TgCRND8 mice overexpressing human APP with Swedish and Indiana familial AD mutations were kindly provided by Dr. George A. Carlson (McLaughlin institute).[35] tTA mice (B6.Cg-Tg(Camk2a-tTA)1Mmay/DboJ) were purchased from the Jackson Laboratory, Bar Harbor, ME. Male APP mice were crossed with female tTA mice to generate APP/tTA (double-positive, defined as AD mice in this study) and non-Tg mice (both negative as age-matched control). All animal studies adhered to the guidelines established by the Institutional Animal Care and Use Committee at University of Nebraska Medical Center.

Stereotaxic injection. Mice at 2 months of age received i.p. injection of ketamine/xylazine for anesthesia (100 mg/kg ketamine and 20 mg/kg xylazine). After mice were immobilized in a stereotaxic microinjection frame (Stoelting, Wood Dale, IL), a linear skin incision was made exposing the bregma, and a 1-mm burr hole was drilled in the skull 2.1 mm posterior and 1.8 mm lateral to the bregma on both sides using a handheld driller (Craftsman). A total volume of 2 μl of saline containing AAV-TRE-GFP or CD74 (1×10^9 vg) was injected into hippocampus using Hamilton syringe (Hamilton, Reno, NV) equipped with 30-gauge needle at 0.2 μl/ min at a depth of 1.8 mm below the skull.

Tissue preparation. Four months postinjection, mice were deeply euthanized with isoflurane and transcardially perfused with 25 ml of ice-cold PBS, followed by 4% paraformaldehyde/PBS (Sigma-Aldrich). The brains were rapidly removed. The left hemisphere was dissected and immediately frozen in dry ice for biochemical testing. The right hemisphere was immersed in freshly depolymerized 4% paraformaldehyde for 48 hours at 4 °C,

and protected by successive 24-hour immersions in 15 and 30% sucrose in 1× PBS. The fixed, cryopreserved brains were sectioned coronally using a Cryostat (Leica, Bannockburn, IL) with sections serially collected and stored at −80 °C for immunohistochemical tests. For biochemical testing, protein extraction of extracellular, intracellular and membrane-enriched fractions and immunoblot tests were performed as described.[20] Protein concentration was determined using Micro BCA Protein Assay (Thermo Fisher Scientific).

ELISA and Immunoblot tests. Protein lysates were subjected to Aβ40 and 42 ELISA (Life Technologies). For immunoblot, protein lysates were diluted 1:1 with Laemmli buffer containing β-mercaptoethanol, incubated at 100 °C for 5 minutes, electrophoresed on 10% sodium dodecyl sulfate-polyacrylamide Tris-Tricine gels[36] and electroblotted to 0.45-μm pore size polyvinylidene difluoride membranes (Immobilon-P, Millipore, Billerica, MA). Membranes were blocked in 5% skim milk/Tris buffered saline containing 0.05% Tween-20, and incubated with CD74 monoclonal (1:100, NB100-78089, Novus Biologicals, Littleton, CO), GFP rabbit polyclonal (1:5,000, Abcam, Cambridge, MA), or APP C-terminal rabbit polyclonal (#171610, 1:1,000, Millipore) at 4 °C for overnight, followed by 30-minute incubation in 5% skim milk/Tris buffered saline containing 0.05% Tween-20 with horseradish peroxidase-conjugated anti-goat or rabbit IgG antibodies (Ab) (1: 2,000, Santa Cruz Biotechnology, Santa Cruz, CA). Immunoreactive bands were detected with SuperSignal West Pico or Femto Chemiluminescent substrate (Thermo Fisher Scientific) and captured using FluorChem M MultiFluor system (ProteinSimple, Santa Clara, CA). After detection of the bands, membranes were incubated with Restore Western Blot Stripping Buffer (Thermo Fisher Scientific) and were then used to detect β-actin for normalization using horseradish peroxidase-conjugated anti-β-actin monoclonal (Sigma). For quantitative analysis, ImageJ software (NIH, Bethesda, MD) was used to quantify band intensities relative to control on captured images.

Immunoprecipitation. Differentiated NPCs were transduced with indicated amounts of AAV2-GFP or AAV2-flag-tagged-CD74, and infected with AdAPPsw, and harvested using ice-cold radioimmunoprecipitation assay buffer with protease inhibitor cocktail as described above. One hundred micrograms of protein/sample were incubated with APP C-terminal rabbit polyclonal (#171610, 1:1,000, Millipore) or Flag monoclonal (Sigma) in radioimmunoprecipitation assay buffer with protease inhibitor cocktail at 4 °C for 1 hour, followed by incubation with 20 μl of Protein A/G Plus agarose (Santa Cruz Biotechnology) at 4 °C for overnight. Precipitants were collected by centrifugation at 3,000 rpm, 4 °C for 5 minutes, washed and reconstituted with Laemmli buffer, incubated at 100 °C for 7 minutes, and then subjected to immunoblots as described above using APP C-terminal rabbit polyclonal and Flag monoclonal.

Immunohistochemistry. Immunohistochemistry was performed as previously described[32] using a specific Ab to identify pan-Aβ (rabbit polyclonal, 1:100, Zymed, San Francisco, CA). Immunodetection was visualized using biotin-conjugated anti-rabbit IgG was used as a secondary Ab, followed by a tertiary incubation with Vectastain ABC Elite kit (Vector Laboratories, Burlingame, CA). For quantification analysis, the areas of Aβ loads were analyzed by ImageJ software (NIH) at 300 μm intervals in ten 30 μm coronal sections from each mouse. Six mouse brains per group were analyzed.

Immunofluorescence. Immunofluorescence was performed using specific Abs to pan-Aβ (rabbit polyclonal, 1:100, Zymed), CD74 (1:50, NB100-78089, Novus Biologicals, Littleton, CO), HA (rat polyclonal, 1:200, Santa Cruz Biotechnology), Rab5, Rab7 (rabbit polyclonal, 1:200, Santa Cruz Biotechnology) and Lamp1 (rabbit polyclonal, ab24170, 1:500, Abcam). Alexa Fluor 488 goat anti-mouse IgG, Alexa Fluor 568 goat anti-rabbit IgG, and Alexa Fluor 647 goat anti-rat IgG (Life Technologies) were used as secondary. Images were captured using a 63× oil lens on a LSM 710 confocal microscope (Carl Zeiss Microimaging, Thornwood, NY). Images were quantified using ImageJ software with a colocalization plugin (http://rsb.info.nih.gov/ij/plugins/colocalization.html) (NIH).

Morris water maze test. The Morris water maze task was utilized to assess spatial learning and memory performance of the mice as described with minor modifications.[37] Mice were introduced into the perimeter of a circular water-filled tank 110 cm in diameter and 91 cm in height (San Diego Instruments, San Diego, CA) with visual cues that were present on the tank walls as spatial references. The tank was divided into four equal quadrants (Q1–4) by lines drawn on the floor. A 10-cm circular plexiglass platform was submerged 1 cm deep in Q2 and as such hidden from the mice. The mice started the task from one of three quadrants Q1, Q3, and Q4, varied by day of testing. Four trials were performed per mouse per day for 10 days. Each trial lasted 1 minute and ended when the mouse climbed onto and remained on the hidden platform for 10 seconds. The mouse was given 20 seconds to rest on the platform between trials. The time taken by the mouse to reach the platform was recorded as its latency. If the mouse did not reach the platform, 60 seconds was recorded as its latency and the mouse was gently guided to the submerged platform. The time for four trials was averaged and recorded as a result for each mouse. On day 11, the mice were subjected to a single 60-second probe trial without platform to test memory retention. The mice started the trial from Q4, number of annulus crossings was counted, and swimming path was recorded using an overhead video camera and Ethovision tracking software (Noldus Information Technology, Leesburg, VA). The percentage of time spent in each quadrant was calculated using the software.

Statistics. All data were normally distributed and presented as mean values ± standard errors of the mean. In the case of single mean comparison, data were analyzed by Student's *t*-test. In case of multiple mean comparisons, the data were analyzed by one-way analysis of variance and Newman-Keuls *post-hoc* or two-way repeated measures analysis of variance, followed by Bonferroni multiple comparison tests using statistics software (Prism 4.0, Graphpad Software, San Diego, CA). A value of $P < 0.05$ was regarded as a significant difference.

SUPPLEMENTARY MATERIAL

Figure S1. Subcellular localization of APP with Rab5 or Rab7 in CD74-overexpressing neurons.

ACKNOWLEDGMENTS

The authors thank George Carlson (McLaughlin Institute) for providing TgCRND8 mice, Kay-Uwe Wagner (University of Nebraska Medical Center) for pUHD15-1, Tsuneya Ikezu (Boston University) for pAdTrack-APPsw, University of Pennsylvania Gene Therapy Program for p5E18RXC1 and pAdΔF6 vectors, Li Wu (University of Nebraska Medical Center) for providing primary cultivated human neurons, and James R. Talaska (Confocal Laser Scanning Core facility, University of Nebraska Medical Center) for assistance with confocal microscopy. This work was supported in part by NIH Grant AG043540, DA028555, NS036126, NS034239, MH064570, NS043985, MH062261, and DOD Grant 421-20-09A to HEG, the Carol Swarts Emerging Neuroscience Fund, start-up funds from the Department of Pharmacology and Experimental Neuroscience, and the Shoemaker Award for Neurodegenerative Research to TK. The authors declare no competing financial interest.

REFERENCES

1. Selkoe, DJ (1991). The molecular pathology of Alzheimer's disease. *Neuron* **6**: 487–498.
2. Hardy, JA and Higgins, GA (1992). Alzheimer's disease: the amyloid cascade hypothesis. *Science* **256**: 184–185.
3. Hardy, J and Selkoe, DJ (2002). The amyloid hypothesis of Alzheimer's disease: progress and problems on the road to therapeutics. *Science* **297**: 353–356.
4. Brody, DL and Holtzman, DM (2008). Active and passive immunotherapy for neurodegenerative disorders. *Annu Rev Neurosci* **31**: 175–193.
5. Lemere, CA (2013). Immunotherapy for Alzheimer's disease: hoops and hurdles. *Mol Neurodegener* **8**: 36.
6. Panza, F, Logroscino, G, Imbimbo, BP and Solfrizzi, V (2014). Is there still any hope for amyloid-based immunotherapy for Alzheimer's disease? *Curr Opin Psychiatry* **27**: 128–137.

7. Haass, C, Kaether, C, Thinakaran, G and Sisodia, S (2012). Trafficking and proteolytic processing of APP. *Cold Spring Harb Perspect Med* **2**: a006270.
8. Rajendran, L and Annaert, W (2012). Membrane trafficking pathways in Alzheimer's disease. *Traffic* **13**: 759–770.
9. Pimplikar, SW, Nixon, RA, Robakis, NK, Shen, J and Tsai, LH (2010). Amyloid-independent mechanisms in Alzheimer's disease pathogenesis. *J Neurosci* **30**: 14946–14954.
10. Pacheco-Quinto, J and Eckman, EA (2013). Endothelin-converting enzymes degrade intracellular β-amyloid produced within the endosomal/lysosomal pathway and autophagosomes. *J Biol Chem* **288**: 5606–5615.
11. Rajendran, L, Honsho, M, Zahn, TR, Keller, P, Geiger, KD, Verkade, P *et al.* (2006). Alzheimer's disease beta-amyloid peptides are released in association with exosomes. *Proc Natl Acad Sci USA* **103**: 11172–11177.
12. Knobloch, M, Farinelli, M, Konietzko, U, Nitsch, RM and Mansuy, IM (2007). Abeta oligomer-mediated long-term potentiation impairment involves protein phosphatase 1-dependent mechanisms. *J Neurosci* **27**: 7648–7653.
13. Oddo, S, Caccamo, A, Kitazawa, M, Tseng, BP and LaFerla, FM (2003). Amyloid deposition precedes tangle formation in a triple transgenic model of Alzheimer's disease. *Neurobiol Aging* **24**: 1063–1070.
14. Beswick, EJ and Reyes, VE (2009). CD74 in antigen presentation, inflammation, and cancers of the gastrointestinal tract. *World J Gastroenterol* **15**: 2855–2861.
15. Basha, G, Omilusik, K, Chavez-Steenbock, A, Reinicke, AT, Lack, N, Choi, KB *et al.* (2012). A CD74-dependent MHC class I endolysosomal cross-presentation pathway. *Nat Immunol* **13**: 237–245.
16. Bryan, KJ, Zhu, X, Harris, PL, Perry, G, Castellani, RJ, Smith, MA *et al.* (2008). Expression of CD74 is increased in neurofibrillary tangles in Alzheimer's disease. *Mol Neurodegener* **3**: 13.
17. Matsuda, S, Matsuda, Y and D'Adamio, L (2009). CD74 interacts with APP and suppresses the production of Abeta. *Mol Neurodegener* **4**: 41.
18. Wang, C, Wang, CM, Clark, KR and Sferra, TJ (2003). Recombinant AAV serotype 1 transduction efficiency and tropism in the murine brain. *Gene Ther* **10**: 1528–1534.
19. Taymans, JM, Vandenberghe, LH, Haute, CV, Thiry, I, Deroose, CM, Mortelmans, L *et al.* (2007). Comparative analysis of adeno-associated viral vector serotypes 1, 2, 5, 7, and 8 in mouse brain. *Hum Gene Ther* **18**: 195–206.
20. Lesné, S, Koh, MT, Kotilinek, L, Kayed, R, Glabe, CG, Yang, A *et al.* (2006). A specific amyloid-beta protein assembly in the brain impairs memory. *Nature* **440**: 352–357.
21. Morgan, D (2011). Immunotherapy for Alzheimer's disease. *J Intern Med* **269**: 54–63.
22. Citron, M (2010). Alzheimer's disease: strategies for disease modification. *Nat Rev Drug Discov* **9**: 387–398.
23. Doraiswamy, PM and Xiong, GL (2006). Pharmacological strategies for the prevention of Alzheimer's disease. *Expert Opin Pharmacother* **7**: 1–10.
24. Maioli, E, Torricelli, C and Valacchi, G (2012). Rottlerin and curcumin: a comparative analysis. *Ann N Y Acad Sci* **1259**: 65–76.
25. Davies, L, Wolska, B, Hilbich, C, Multhaup, G, Martins, R, Simms, G *et al.* (1988). A4 amyloid protein deposition and the diagnosis of Alzheimer's disease: prevalence in aged brains determined by immunocytochemistry compared with conventional neuropathologic techniques. *Neurology* **38**: 1688–1693.
26. Mann, DM, Jones, D, South, PW, Snowden, JS and Neary, D (1992). Deposition of amyloid beta protein in non-Alzheimer dementias: evidence for a neuronal origin of parenchymal deposits of beta protein in neurodegenerative disease. *Acta Neuropathol* **83**: 415–419.
27. LaFerla, FM, Green, KN and Oddo, S (2007). Intracellular amyloid-beta in Alzheimer's disease. *Nat Rev Neurosci* **8**: 499–509.
28. Gouras, GK, Tampellini, D, Takahashi, RH and Capetillo-Zarate, E (2010). Intraneuronal beta-amyloid accumulation and synapse pathology in Alzheimer's disease. *Acta Neuropathol* **119**: 523–541.
29. Starlets, D, Gore, Y, Binsky, I, Haran, M, Harpaz, N, Shvidel, L *et al.* (2006). Cell-surface CD74 initiates a signaling cascade leading to cell proliferation and survival. *Blood* **107**: 4807–4816.
30. Shachar, I and Haran, M (2011). The secret second life of an innocent chaperone: the story of CD74 and B cell/chronic lymphocytic leukemia cell survival. *Leuk Lymphoma* **52**: 1446–1454.
31. Stone, DK, Kiyota, T, Mosley, RL and Gendelman, HE (2012). A model of nitric oxide induced α-synuclein misfolding in Parkinson's disease. *Neurosci Lett* **523**: 167–173.
32. Kiyota, T, Ingraham, KL, Jacobsen, MT, Xiong, H and Ikezu, T (2011). FGF2 gene transfer restores hippocampal functions in mouse models of Alzheimer's disease and has therapeutic implications for neurocognitive disorders. *Proc Natl Acad Sci USA* **108**: E1339–E1348.
33. Peng, H, Huang, Y, Rose, J, Erichsen, D, Herek, S, Fujii, N *et al.* (2004). Stromal cell-derived factor 1-mediated CXCR4 signaling in rat and human cortical neural progenitor cells. *J Neurosci Res* **76**: 35–50.
34. Ikezu, T, Luo, X, Weber, GA, Zhao, J, McCabe, L, Buescher, JL *et al.* (2003). Amyloid precursor protein-processing products affect mononuclear phagocyte activation: pathways for sAPP- and Abeta-mediated neurotoxicity. *J Neurochem* **85**: 925–934.
35. Chishti, MA, Yang, DS, Janus, C, Phinney, AL, Horne, P, Pearson, J *et al.* (2001). Early-onset amyloid deposition and cognitive deficits in transgenic mice expressing a double mutant form of amyloid precursor protein 695. *J Biol Chem* **276**: 21562–21570.
36. Schägger, H (2006). Tricine-SDS-PAGE. *Nat Protoc* **1**: 16–22.
37. Arendash, GW, Schleif, W, Rezai-Zadeh, K, Jackson, EK, Zacharia, LC, Cracchiolo, JR *et al.* (2006). Caffeine protects Alzheimer's mice against cognitive impairment and reduces brain beta-amyloid production. *Neuroscience* **142**: 941–952.